



Hollow-core infrared fiber incorporating metal-wire metamaterial

Yan, Min; Mortensen, N. Asger

Published in:
Optics Express

Link to article, DOI:
[10.1364/OE.17.014851](https://doi.org/10.1364/OE.17.014851)

Publication date:
2009

Document Version
Publisher's PDF, also known as Version of record

[Link back to DTU Orbit](#)

Citation (APA):
Yan, M., & Mortensen, A. (2009). Hollow-core infrared fiber incorporating metal-wire metamaterial. *Optics Express*, 17(17), 14851-14864. DOI: 10.1364/OE.17.014851

General rights

Copyright and moral rights for the publications made accessible in the public portal are retained by the authors and/or other copyright owners and it is a condition of accessing publications that users recognise and abide by the legal requirements associated with these rights.

- Users may download and print one copy of any publication from the public portal for the purpose of private study or research.
- You may not further distribute the material or use it for any profit-making activity or commercial gain
- You may freely distribute the URL identifying the publication in the public portal

If you believe that this document breaches copyright please contact us providing details, and we will remove access to the work immediately and investigate your claim.

Hollow-core infrared fiber incorporating metal-wire metamaterial

Min Yan* and Niels Asger Mortensen†

Department of Photonics Engineering,
Technical University of Denmark, DK-2800 Kongens Lyngby, Denmark

* miyan@fotonik.dtu.dk, † asger@mailaps.org

Abstract: Infrared (IR) light is considered important for short-range wireless communication, thermal sensing, spectroscopy, material processing, medical surgery, astronomy etc. However, IR light is in general much harder to transport than optical light or microwave radiation. Existing hollow-core IR waveguides usually use a layer of metallic coating on the inner wall of the waveguide. Such a metallic layer, though reflective, still absorbs guided light significantly due to its finite Ohmic loss, especially for transverse-magnetic (TM) light. In this paper, we show that metal-wire based metamaterials may serve as an efficient TM reflector, reducing propagation loss of the TM mode by two orders of magnitude. By further imposing a conventional metal cladding layer, which reflects specifically transverse-electric (TE) light, we can potentially obtain a low-loss hollow-core fiber. Simulations confirm that loss values for several low-order modes are comparable to the best results reported so far.

© 2009 Optical Society of America

OCIS codes: (060.2310) Fiber optics; (060.2280) fiber design and fabrication; (160.3918) metamaterials; (240.6680) surface plasmons; (240.5420) polaritons.

References and links

1. J. A. Harrington, "A review of IR transmitting, hollow waveguides," *Fiber Integrated Opt.* **19**, 211–217 (2000).
2. B. Temelkuran, S. D. Hart, G. Benoit, J. D. Joannopoulos, and Y. Fink, "Wavelength-scalable hollow optical fibres with large photonic bandgaps for CO₂ laser transmission," *Nature* **420**, 650–653 (2002).
3. R. F. Cregan, B. J. Mangan, J. C. Knight, T. A. Birks, P. S. J. Russell, P. J. Roberts, and D. C. Allan, "Single-mode photonic band gap guidance of light in air," *Science* **285**, 1537–1539 (1999).
4. B. Bowden, J. A. Harrington, and O. Mitrofanov, "Low-loss modes in hollow metallic terahertz waveguides with dielectric coatings," *Appl. Phys. Lett.* **93**, 181104 (2008).
5. B. T. Schwartz and R. Piestun, "Waveguiding in air by total external reflection from ultralow index metamaterials," *Appl. Phys. Lett.* **85**, 1 (2004).
6. E. J. Smith, Z. Liu, Y. Mei, and O. G. Schmidt, "Combined surface plasmon and classical waveguiding through metamaterial fiber design," *Nano Lett.*, DOI:10.1021/nl900550j (2009).
7. J. Elser, R. Wangberg, V. A. Podolskiy, and E. E. Narimanov, "Nanowire metamaterials with extreme optical anisotropy," *Appl. Phys. Lett.* **89**, 261102 (2006).
8. Y. Liu, G. Bartal, and X. Zhang, "All-angle negative refraction and imaging in a bulk medium made of metallic nanowires in the visible region," *Opt. Express* **16**, 15439–15448 (2008). URL <http://www.opticsexpress.org/abstract.cfm?URI=oe-16-20-15439>.
9. J. B. Pendry, A. J. Holden, W. J. Stewart, and I. Youngs, "Extremely low frequency plasmons in metallic mesostructures," *Phys. Rev. Lett.* **76**, 4773 (1996).
10. J. Yao, Z. Liu, Y. Liu, Y. Wang, C. Sun, G. Bartal, A. M. Stacy, and X. Zhang, "Optical negative refraction in bulk metamaterials of nanowires," *Science* **321**, 930 (2008).
11. D. R. Smith and D. Schurig, "Electromagnetic wave propagation in media with indefinite permittivity and permeability tensors," *Phys. Rev. Lett.* **90**, 077405 (2003).
12. E. Hecht, *Optics*, 4th ed. (Addison Wesley, San Francisco, 2002).

13. E. D. Palik, *Handbook of Optical Constants of Solids* (Academic Press, New York, 1985).
 14. M. Yan and P. Shum, "Analysis of perturbed Bragg fibers with an extended transfer matrix method," *Opt. Express* **14**, 2596–2610 (2006). URL <http://www.opticsexpress.org/abstract.cfm?URI=oe-14-7-2596>.
 15. S. Quabis, R. Dorn, M. Eberler, O. Glöckl, and G. Leuchs, "Focusing light to a tighter spot," *Opt. Comm.* **179**, 1–7 (2000).
 16. E. A. J. Marcatili and R. A. Schmeltzer, "Hollow metallic and dielectric waveguides for long distance optical transmission and lasers," *Bell Syst. Tech. J.* **34**, 1783–1809 (1964).
 17. S. Johnson, M. Ibanescu, M. Skorobogatiy, O. Weisberg, T. Engeness, M. Soljacic, S. Jacobs, J. Joannopoulos, and Y. Fink, "Low-loss asymptotically single-mode propagation in large-core OmniGuide fibers," *Opt. Express* **9**, 748–779 (2001). URL <http://www.opticsexpress.org/abstract.cfm?URI=oe-9-13-748>.
-

1. Introduction

Waveguides for infrared (IR) light are most often inferior as compared to those for optical or microwave light. In general the lack of excellent transparent solids at IR wavelength calls for hollow-core guidance rather than solid-core guidance relying on total internal reflection (TIR). While presently the latter solution remains attractive for single-mode light guidance usually over a short distance, extension of such a solid-core IR fiber to high-power light guidance is difficult due to adverse effects including Fresnel loss, thermal lensing, and low damage threshold power, etc. Without TIR, hollow-core fibers require a highly-reflective cladding mirror. At the moment, there are mainly two recognized hollow-core IR waveguiding structures, either relying on reflective metal mirrors [1] or a dielectric photonic band-gap (PBG) material [2] which was first explored for guiding light at optical wavelengths over the past decade [3]. Unlike at microwave wavelength, metals at IR wavelength are less perfectly reflecting mirrors due to the presence of finite Ohmic absorption. Hence a direct IR waveguiding using a hollow metallic fiber (HMF) does not work well. The same dilemma exists for the transport of terahertz electromagnetic (EM) waves, i.e. far-IR light (refer to [4] and references therein). In practice, it is necessary to further refine the HMF by adding an additional dielectric coating on the metal cladding [1, 4]. PBG guidance on the other hand remains as a potential solution, but the guiding mechanism is inherently band-gap limited and heavily relies on a highly periodic photonic crystal cladding. Bragg fibers with a $700\ \mu\text{m}$ -diameter core have facilitated hollow-core band-gap guidance of CO_2 laser radiation ($10.6\ \mu\text{m}$) with a propagation loss of $\sim 1\ \text{dB/m}$ [2]. The state-of-the-art HMF with a dielectric coating with the same core size experiences a similar loss level at this wavelength [1].

In this paper, we show that metamaterials hold promises for entirely new guiding mechanisms, being of neither PBG nature nor relying on the classical TIR. In fact, the potential of especially metal-based metamaterial has already been exploited for novel hollow-core planar waveguide [5] and fiber [6] designs. In the present work, we propose a hybrid mirror consisting of a first metal-wire metamaterial layer and a second plain metal layer for achieving hollow-core IR guidance. The first layer reflects specifically transverse-magnetic (TM) light, while the second reflects transverse-electric (TE) light. TM reflection by the first metamaterial layer is based on the fact that a highly anisotropic medium with different signs in its effective permittivity tensor components is able to totally reflect TM light. This mechanism is fundamentally different from the previous proposals [5, 6] in which the confinement in a hollow core is due to a metamaterial cladding with an effective refractive index between 0 and 1. The metamaterial deployed in our fiber can provide better reflection for TM light than a plain metal, which helps to reduce the losses of the TM modes in the proposed fiber. Existing hollow-core IR fibers including both Bragg fibers and HMFs have a common drawback of suffering from very high losses for the TM modes (several orders of magnitude as high as those experienced by the TE modes). Our deployment of the metamaterial layer therefore addresses this critical drawback by bringing down the losses of the TM modes close to those experienced by the TE modes.

The paper is organized as follows. First, in Section 2 we will show why a planar interface between a metal-wire metamaterial and air can serve as a mirror for the TM-polarized light at IR frequency. The condition required for such a total external reflection is stated. We quantitatively derive the angular reflectance spectrum for a silver-wire medium approximated as a homogeneous medium with an effective medium theory (EMT), proving its superior reflection performance at large incidence angles compared to a bulk silver. In Section 3, we study hollow-core IR guidance in cylindrical fibers with a metal-wire medium as cladding. The fiber, which converges to a traditional HMF when the fraction of metal increases, has a drastically improved performance over HMF, as we will support by calculations based on both EMT as well as rigorous full-vectorial finite-element simulations accounting for the mesoscopic structure of the cladding metamaterial. In Section 4, we briefly compare how our proposed metamaterial fiber differs with a HMF with a dielectric inner coating. Finally, discussion and conclusion are presented in Section 5.

2. Planar geometry

2.1. Why does it reflect?

The planar geometry serves as a simple yet clear example explaining why a metal-wire based metamaterial can easily form a reflector for TM light at IR frequency. Figure 1(a) describes a semi-infinite metamaterial formed by z -oriented metal wires imbedded in a host dielectric occupying a half-space, say $x < 0$. When the wire diameter and wire separation are much smaller than the operating wavelength, the composite can be conveniently treated as a homogeneous medium with an effective permittivity tensor of the diagonal form $\bar{\epsilon} = \text{diag}(\epsilon_x, \epsilon_y, \epsilon_z)$ while for the permeability the medium appears isotropic with $\mu = 1$. For uniformly dispersed wires we have $\epsilon_x = \epsilon_y \equiv \epsilon_t$. When the size of metal wires is close to the skin depth of the metal (tens of nanometers), the Maxwell-Garnett theory (MGT) is adequate, especially at small metal filling fraction, for deriving the effective permittivity tensor of the homogenized metamaterial [7, 8],

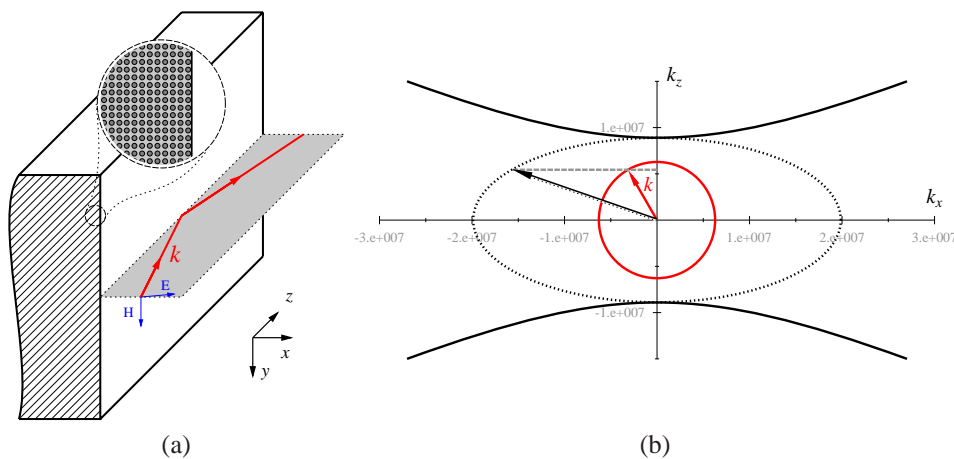


Fig. 1. (a) Metal-wire medium as a TM reflector in planar geometry. (b) $k_x \sim k_z$ relations for TM light in both air (red curve) and an indefinite medium with $\epsilon_x = 2, \mu_y = 1, \epsilon_z = -10$ (black curves), together with wavevectors illustrating reflection for TM light incidence. Axis unit: rad/m. $\lambda = 1 \mu\text{m}$.

i.e.

$$\epsilon_t = \epsilon_d + \frac{f_m \epsilon_d (\epsilon_m - \epsilon_d)}{\epsilon_d + 0.5 f_d (\epsilon_m - \epsilon_d)} \quad (1a)$$

$$\epsilon_z = f_m \epsilon_m + f_d \epsilon_d, \quad (1b)$$

where f_d and f_m represent filling ratios of the dielectric and metallic materials ($f_d + f_m = 1$), respectively; ϵ_d and ϵ_m are the permittivity values of the element dielectric and metallic materials, respectively. As shown by Eq. (1), the effective permittivity components are solely determined by f_m . The component ϵ_z is usually negative due to un-restricted electron motion in the z direction, while ϵ_t is usually positive [7–10]. Such a metamaterial with both positive and negative material tensor components is referred to as an *indefinite medium* [11].

In Fig. 1(a), we schematically show that a metal-wire medium totally reflects a TM-polarized light (with field components E_x , H_y , and E_z) incident from air, with its wavevector lying in the xz plane. Before setting out to investigate the reflection conditions, we show how the total reflection is possible with a rather common indefinite medium fulfilling the very first requirement

$$\epsilon_x > 0, \mu_y > 0, \epsilon_z < 0. \quad (\text{requirement 1}) \quad (2)$$

The medium chosen has $\epsilon_x = 2, \mu_y = 1, \epsilon_z = -10$ (a typical effective medium realizable with metal wires). Notice that only three material parameters are relevant to TM-polarized light.

When a TM wave is propagating in the xz plane of a general medium, the dispersion relation of the wave is governed by

$$\frac{k_z^2}{\epsilon_x} + \frac{k_x^2}{\epsilon_z} = k_0^2 \mu_y, \quad (3)$$

where $k_0 = \omega/c$ is the free-space wave number. In a waveguide picture where the EM field is propagating along the z direction, k_z is also called propagation constant β which is required to be real. For EM wave propagating in an ordinary isotropic dielectric medium, the eligible real (k_z, k_x) combinations form a circle on the k_z - k_x plane, as shown in Fig. 1(b) for the case of vacuum. However, for an indefinite medium defined by Eq. (2), Eq. (3) becomes a hyperbolic equation with real k_x if $k_z > k_c$, where $k_c = \sqrt{\epsilon_x (k_0^2 \mu_y - k_x^2 / \epsilon_z)}$, or otherwise an elliptic equation with imaginary k_x . For a waveguiding purpose, we always desire an imaginary k_x in order for the field to be evanescent along the lateral x direction (a wave propagating along z while evanescent along x is therefore a surface wave). Figure 1(b) shows the $k_x \sim k_z$ dispersion relation for the above-mentioned representative indefinite medium. As indicated by Fig. 1(b), the incident light from air (red arrow) can easily be matched in the tangential k component (k_z) by a surface wave in the indefinite medium (solid-dotted arrow). Therefore, the medium reflects TM light with k lying in the xz plane. It follows that a hollow-core slab waveguide with two claddings made of such media is able to propagate TM light.

Based on the dispersion diagram in Fig. 1(b), we address a further requirement in order for the total reflection to happen *at all incidence angles* in the xz incidence plane. That is, the hyperbola should not touch the red circle, otherwise at large incidence angles, the k_z component of the incident light can be matched by a propagating wave in the indefinite medium. That is, light would transmit through the substrate. This imposes $k_0^2 \epsilon_x \mu_y > k_0^2$, or simply

$$\epsilon_x \mu_y > 1, \quad (\text{requirement 2}) \quad (4)$$

which should be enforced on top of requirement 1.

Putting the two requirements together, we obtain a relaxed (but sufficient) condition for a medium possessing all-angle reflection (in the xz incidence plane) for TM light, as

$$\epsilon_x > 1, \mu_y = 1, \epsilon_z < 0. \quad (5)$$

This condition is rather easy to be fulfilled with a metal-wire medium. For instance, based on MGT approximation, silver wires in a dielectric host with any permittivity from 2 to 12, and with any metal filling fraction from 10% to 50%, will be able to satisfy the above condition from wavelength at $2\mu\text{m}$ and beyond. This suggests the broad structural and spectral applicability of our proposed reflector and in turn waveguide designs.

2.2. How well does it reflect?

Having understood the all-angle reflection for k lying in the xz plane, our next immediate task is to know how high the reflection is. Using a full-wave analytical technique [12], we examine how the reflectance of such a metamaterial substrate is compared to that of a plain metal for TM light. In this paper we concentrate primarily on the CO_2 laser wavelength, i.e. $10.6\mu\text{m}$. This wavelength is important especially due to the fact that high-power CO_2 laser beams can be used for material processing and various medical surgeries. For the wires we consider the use of silver with $\epsilon = -2951 + 1654i$ [13], imbedded in a host dielectric with a refractive index of 2.5 corresponding to $\epsilon = 6.25$. Several transparent materials at this wavelength have their indices around this value, such as zinc selenide (ZnSe) and arsenic selenide (As_2Se_3). We consider a metamaterial in which silver wires take up a volumetric fraction of 20%.

By Eq. (1), the metamaterial under consideration can be effectively treated as a homogeneous medium with $\epsilon_t = 9.3876 + 0.0071i$ and $\epsilon_z = -585.2 + 330.8i$, i.e. an indefinite medium. Using this approximation, the reflectance by the metamaterial-air interface as a function of incidence angle is derived in Fig. 2(a). The wavevector of the incoming plane wave is in the xz plane. The same reflectance curve is derived for a plain silver substrate. Both reflectance curves are characterized by a *principal angle-of-incidence* [12], where the reflectance is at minimum. By comparison, it is noticed that the reflectance of the indefinite medium is lower than that of the plain metal for most incidence angles. However, as clearly shown by the zoom-in plot in Fig. 2(b), at large incidence angles (greater than 88.6 degree) the metamaterial reflects better. In a large-core hollow waveguide, modes in the lowest orders indeed correspond to near-90 degree incidence angles, as will be confirmed in the next section. Therefore, a metal-wire medium can be potentially used for making a less lossy hollow waveguide as compared to using plain metal.

However, the metal-wire medium has difficulty in confining TE light, since the metamaterial

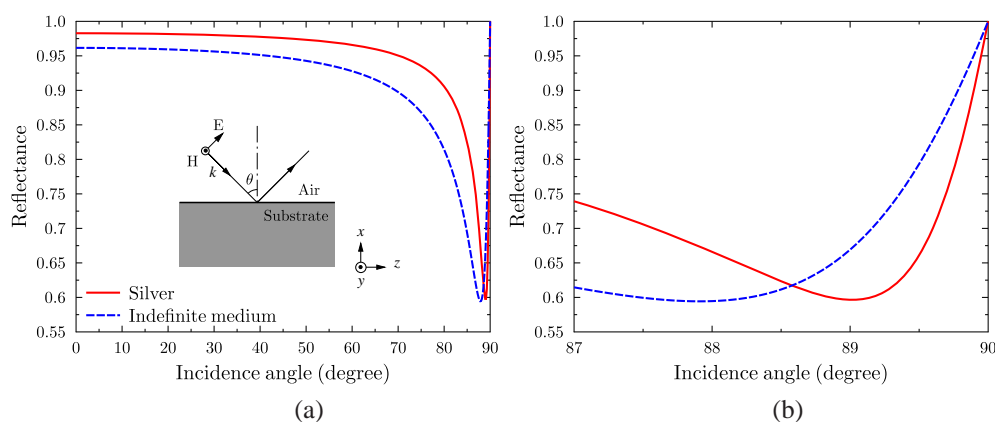


Fig. 2. Reflectance of TM-polarized incident light from two types of substrates, one silver and the other an indefinite medium derived from silver-wire-in-dielectric composite (inset). The wavelength is $10.6\mu\text{m}$. (a) Reflectance spectrum for $0 \sim 90$ degrees; (b) Zoom-in plot for $87 \sim 90$ degrees.

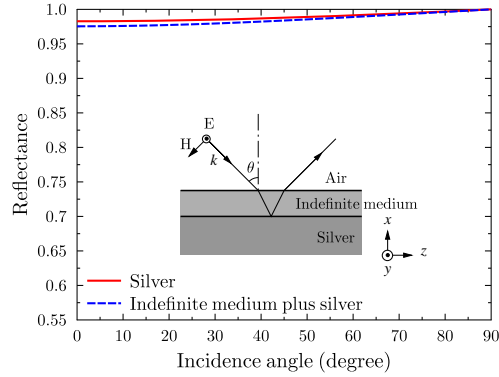


Fig. 3. Reflectance of TE-polarized incident light from two types of substrates, one plain silver and the other silver but with an indefinite medium layer on top (inset). The wavelength is $10.6\mu\text{m}$.

appears to TE light as if it is a normal dielectric. To remedy the problem, we further add a metal substrate beneath the metamaterial. In Fig. 3, we show the reflectance from such a hybrid substrate. The metamaterial layer is the same as that we considered in Fig. 2 and has a thickness of $2\mu\text{m}$. The reflectance spectrum is compared to that from a plain silver substrate, also shown in Fig. 3. It is observed that by adding a layer of metamaterial the reflectance decreases only very slightly, with reflectance still higher than 99.89% when incidence angle is larger than 87° . From Figs. 2 and 3, one also sees that a plain silver surface reflects TE light much better than TM light, especially at large incidence angles.

3. Fiber geometry

3.1. Proposed structure and confinement condition

It is relatively straightforward to understand that the metal-wire medium discussed in Section 2 can be rolled into a fiber geometry, with the metal wires running along the fiber axis, to propagate TM light in a hollow core [see Fig. 4(a)]. Now the TM light, in the fiber's native cylindrical coordinate, consists of E_r , H_θ , and E_z field components. Here to be more rigorous, we rederive the material requirement for the confinement in a cylindrical coordinate system.

For a fiber with an air core, one can derive the most general requirement for achieving TM field confinement (see appendix), expressed in terms of the cladding material parameters, as

$$\frac{\varepsilon_z}{\varepsilon_t} (k_0^2 \mu_t \varepsilon_t - \beta^2) < 0. \quad (6)$$

Here, β is the propagation constant of a confined mode while μ_t and ε_t are cladding material parameters defined as $\varepsilon_r = \varepsilon_\theta \equiv \varepsilon_t$ and $\mu_r = \mu_\theta \equiv \mu_t$. Similarly, the requirement for TE (with field components H_r , E_θ , and H_z) confinement is

$$\frac{\mu_z}{\mu_t} (k_0^2 \varepsilon_t \mu_t - \beta^2) < 0. \quad (7)$$

Note that a guided mode in a hollow-core should have $\beta < k_0$. Apparently there are several combinations of ε_t , ε_z , μ_t and μ_z which fulfil the inequalities in Eqs. (6) and (7). Bulk metal (i.e. $\varepsilon < 0$ and $\mu = 1$) is of course a solution. In relating to the metal-wire metamaterial, we identify another set of solutions specifically for TM confinement, which is

$$\varepsilon_t > 1, \mu_t = 1, \varepsilon_z < 0. \quad (8)$$

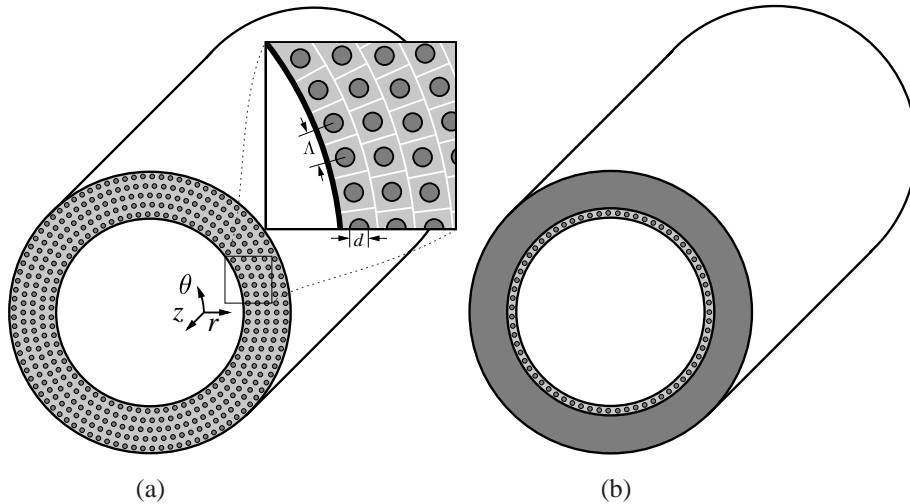


Fig. 4. Schematic diagrams for the proposed metal-wire metamaterial fiber structures. (a) A hollow-core fiber with a metal-wire based metamaterial cladding. Thin white lines in the inset indicate unit cells forming the metamaterial. (b) A hybrid-clad fiber: A hollow-core fiber with a thin layer of metamaterial as its inner cladding, and a bulk metal as its outer cladding. Dark grey regions are metal. Light grey region denotes dielectric material.

Notice Eq. (8) agrees perfectly with Eq. (5). A similar solution exists for TE confinement, namely $\mu_t > 1$, $\epsilon_t = 1$ and $\mu_z < 0$. It is so far difficult to realize a low-loss metamaterial fulfilling this TE confinement condition. In addition, plain metal is already an excellent TE reflector, as concluded in Subsection 2.2. As will be shown later, the propagation loss of the TE_{01} mode can easily be 1000 times smaller than that of the TM_{01} mode in a HMF. Therefore, another choice of TE reflector at a higher expense is unwarranted.

The fiber structure we are to propose takes advantages of both a metal-wire medium for reflection of TM light and a plain metal for reflection of TE light. A schematic diagram of the fiber is shown in Fig. 4(b). The fiber cladding consists of a thin layer of metamaterial for reflecting TM light and another plain metal layer for reflecting TE light. Notice that TE light is perturbed only very slightly by the presence of the metamaterial layer, as implied by Fig. 3. We refer to this fiber as a *hybrid-clad fiber*. For practical realizations, the fiber structure may be coated with an outer jacket for better mechanical stability and ease of handling.

3.2. Numerical results

In our numerical characterization, we first turn attention to the fiber illustrated in Fig. 4(a), whose cladding is all metamaterial. The metal wires (diameter d) in the metamaterial are arranged in annular layers, supported by a dielectric host. In our study cases, the metamaterial can be approximately considered as a stack of square cells [inset in Fig. 4(a)] with a cell separation Λ . For such stacking, the filling fraction of metal wires can reach up to ~ 0.785 .

Normally in a hollow-core fiber (either HMF or Bragg fiber) with a relatively large core size, there are normally a huge number of propagating modes. Among the modes, the TE_{01} mode is recognized as the least lossy one [4]; the first mixed-polarization MP_{11} mode, or traditionally known as the HE_{11} mode, is most useful for power delivery applications, due to its close resemblance to a laser output beam both in intensity profile and polarization; TM modes are the most lossy ones. MP modes have both TE and TM polarization components, therefore a MP mode usually has a propagation loss larger than that of a TE mode but smaller than that of a

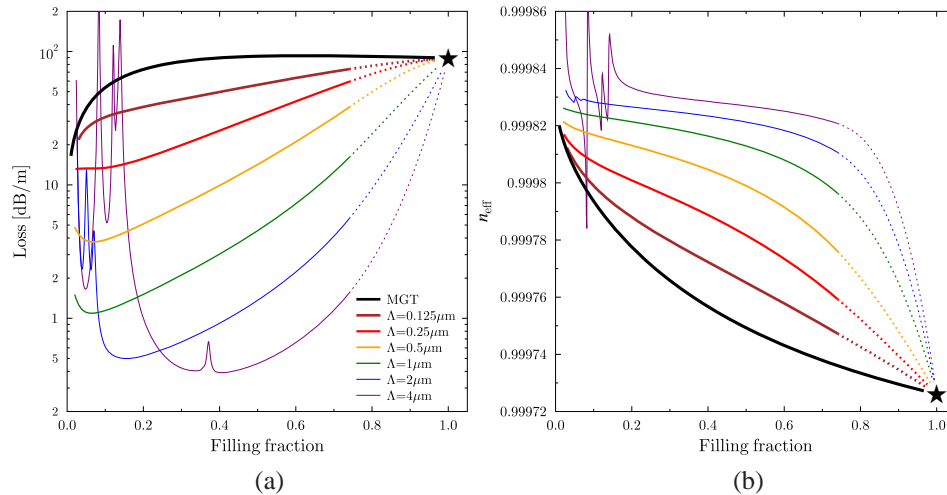


Fig. 5. (a) Propagation loss, and (b) effective mode index of the TM_{01} mode as a function of metal filling fraction. The values for the mode when cladding is made of full metal are marked as \star .

TM mode when the modes under comparison belong to the same mode group (refer to [14] for quantitative loss values derived for the MP_{21} , TE_{01} , and TM_{01} modes in a Bragg fiber). In this paper it is of high priority to address the improved performance of TM modes especially the TM_{01} mode with our metamaterial fiber design. The reason for our focus on the TM polarization is twofold: firstly, a fiber with less lossy TM modes will generally also have less lossy MP modes, as will be shown by our numerical calculations; secondly, the TM_{01} mode is valuable in its own right for certain uses, despite not suitable for laser beam delivery. The TM_{01} mode has an annular beam shape and a radially-oriented electric field, which allows it to be focused into a tighter spot (compared to a linearly polarized beam) with a large longitudinal electric field component at the focus [15]. This property can be exploited for imaging or material processing, etc.

We consider a fiber with an all-metamaterial cladding and a core with diameter of $700 \mu\text{m}$. With a homogenized material based on the MGT approximation, we are able to quite efficiently derive the guided TM_{01} mode properties, including its loss and effective mode index (n_{eff}). The mode properties are plotted against f_m varying from ~ 0 (completely dielectric) to 1 (completely metal) in Fig. 5. It should be remarked that the accuracy of MGT might be questionable at large f_m values. Nevertheless, the results based on MGT agree well with the results calculated by rigorous numerical simulations, as will be shown shortly. It is seen from Fig. 5(a) that, as f_m decreases, the loss value initially remains close to that for the metal-clad fiber, and it drops sharply when f_m becomes less than 0.2. It suggests that it is possible for the metamaterial cladding to perform better than a full-metal cladding for confining the TM mode.

In practice the limit where MGT is valid, i.e. wire diameter comparable to skin depth, is rather difficult to achieve. Here we numerically simulate realistic fiber structures by taking all mesoscopic geometrical features into account. A finite element method (FEM) has been employed for this purpose. Simulations for a number of realistic structures are summarized in Fig. 5, where we show the loss and n_{eff} values of the TM_{01} mode as a function of f_m when the wire spacing Λ takes values of 0.125, 0.25, 0.5, 1, 2, and $4 \mu\text{m}$. Notice that FEM simulations for all curves corresponding to realistic microstructured fibers start from $f_m = 0.02$ and stop at $f_m = 0.74$. Further beyond that filling fraction, the values (dotted portions of the curves) are ex-

trapolated according to the simulated data. It is observed that, when Λ gets larger, the loss curve shifts away from the limiting MGT curve, downwards to smaller values. This further evidences that the metal-wire based metamaterial makes a superior reflector for TM light compared to a plain metal. However, we notice that the downward shift in loss curve is not without limit. In particular, when Λ increases to a certain value (after $2\mu\text{m}$ in this case), the spacings between two neighboring layers of metal wires become large enough to support resonant modes. These modes experience relatively high loss due to their proximity to metal wires. The coupling from the TM_{01} core mode to these cladding resonances will result in higher loss to the TM_{01} mode, which are manifested by the loss spikes observed in Fig. 5(a). These resonances will become especially severe for a large Λ value. From Fig. 5, it is concluded that one should take a compromise between the propagation loss and the number of cladding resonances in choosing the right Λ (and thereafter d). We should mention that it is difficult for the guided core mode to be resonant with surface plasmon polaritons (SPPs) supported by the individual metal wires, as the SPP guided by a single wire has $n_{\text{eff}} > 2.5$ which is significantly larger than n_{eff} of the core mode. From Fig. 5(b), it is shown that the n_{eff} value is larger at smaller f_m values, generally around 0.99982. The corresponding incidence angle for guided light can be estimated, through $\theta = \sin^{-1}(\beta/k_0) = \sin^{-1}(n_{\text{eff}})$, to be $\sim 88.9^\circ$. This is consistent with the reflectance spectrum shown in Fig. 2, in which at the particular incidence angle an improved reflection by a metal-wire metamaterial is predicted.

Here we remark that, for all microstructured metamaterial fiber simulations in Fig. 5 (excluding the homogenized fiber case in the MGT limiting form), we used five layers of metal wires in the cladding, beyond which we have air background. When $\Lambda = 0.125\mu\text{m}$, the metamaterial cladding is as thin as $0.625\mu\text{m}$ (16 times smaller than $10.6\mu\text{m}$). Quite remarkably, such a metamaterial cladding, though very thin, confines TM light exceptionally well. In Fig. 6(a), we show the field distribution of the guided TM_{01} mode. It is noticed that the overall mode field is

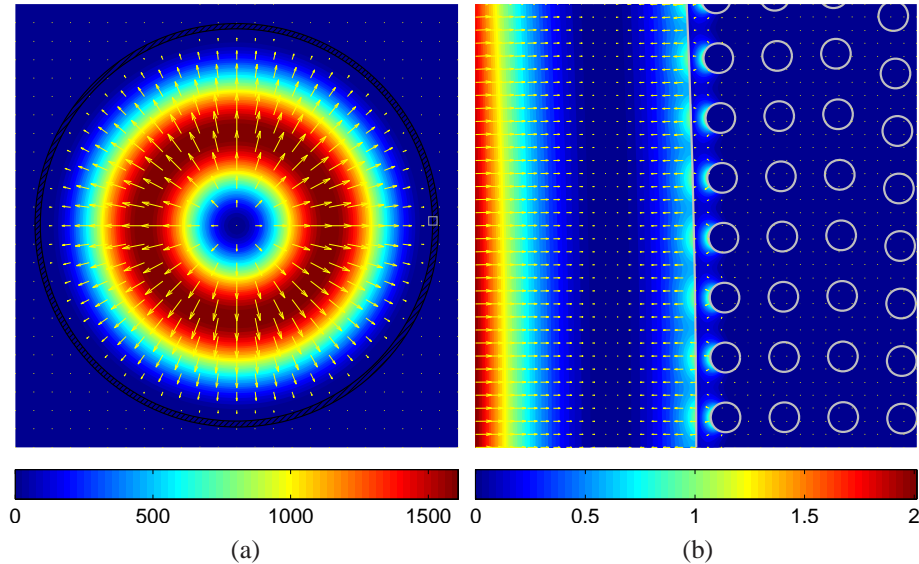


Fig. 6. Cross-sectional field distribution of the guided TM_{01} mode in a metamaterial-clad fiber with a $700\mu\text{m}$ core diameter. (a) Overall mode; (b) The zoom-in plot of the region outlined in (a) by the gray line ($15 \times 15\mu\text{m}^2$). Color shading is for the real part of the axial Poynting vector, while arrows are for transverse electric field. $\lambda = 10.6\mu\text{m}$, $\Lambda = 2\mu\text{m}$, $f_m = 0.2$.

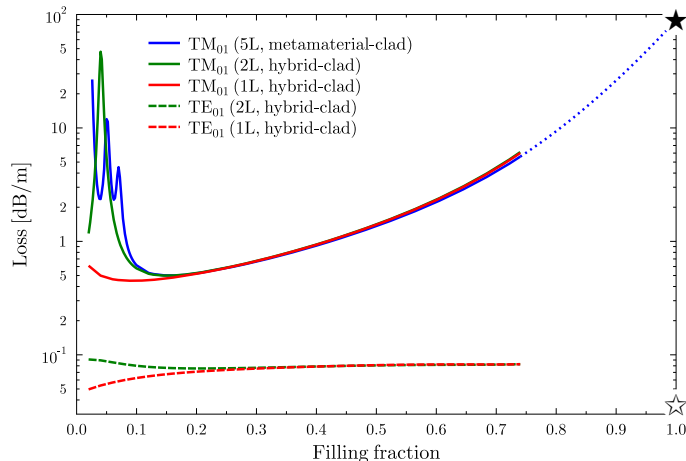


Fig. 7. Propagation losses of both TM_{01} and TE_{01} modes as a function of metal filling fraction. $\lambda = 10.6\mu\text{m}$, $\Lambda = 2\mu\text{m}$. The propagation loss values for the TM_{01} and TE_{01} modes at the $f_m = 1$ limit are marked as \star and \star , respectively.

well guided by the metamaterial cladding. The zoom-in plot in Fig. 6(b) reveals detailed field interaction with the metal-wire medium. The *partially excited* SPPs at metal wires adjacent to the interface imply the anti-resonant nature of the cladding metamaterial. The cladding field macroscopically resembles an evanescent wave which rapidly decays away from the core. The plot also quantitatively indicates that a couple of metal-wire layers would be sufficient to prevent leakage of the TM light. In other words, the metamaterial cladding behaves like a metal to the TM light, and it has a very small (sub-micron) *effective skin depth*.

The fiber in Fig. 4(a), though supporting TM modes, does neither confine TE modes nor MP modes. The hybrid-clad fiber with two claddings in Fig. 4(b) remedies the problem. Among the two claddings, the inner one is of special importance. Based on our results in Fig. 5, here we focus on a particular metal-wire spacing $\Lambda = 2\mu\text{m}$. First we investigate the effect of the metamaterial cladding thickness by studying two hybrid-clad fibers: one has a metamaterial thickness of $2\mu\text{m}$ (one layer of metal wires); the other has a metamaterial thickness of $4\mu\text{m}$ (two layers of metal wires). The loss values for the TE_{01} and TM_{01} modes guided by the two fibers are shown in Fig. 7, expressed again as functions of f_m . We also superposed the loss curve of the TM_{01} mode guided by a fiber with pure metamaterial cladding [i.e. the curve marked with “ $\Lambda = 2\mu\text{m}$ ” in Fig. 5(a)]. According to Fig. 7, at a relatively large f_m value the TM_{01} mode loss is hardly affected as compared to the value for the metamaterial-clad fiber, which is true even when the hybrid-clad fiber has only one layer of metal wires. At small f_m , a thin metamaterial cladding layer even helps to reduce the cladding resonance, and therefore to reduce the loss of the TM_{01} mode. It turns out that the lowest loss for the TM_{01} mode is achieved by the hybrid-clad fiber with only one layer of metal wires. In the limit of $f_m = 1.0$, both hybrid fibers degenerate into a HMF, whose TM_{01} and TE_{01} modes have loss values as indicated by the black and open stars, respectively, in Fig. 7. Clearly we see that in such a conventional HMF, the TM mode suffers over 1000 times higher loss as compared to the TE mode. This is the key factor that restricts the usage of such a conventional fiber at this operating wavelength.

By adding a metamaterial layer as an inner cladding, the TE_{01} mode is found to have a slightly higher loss as compared to that in a HMF of the same core size. However, the loss value of the TE_{01} mode is still below 0.1 dB/m, which is well acceptable for a wide range of applications. No cladding resonance have been found in this particular case which deteriorates

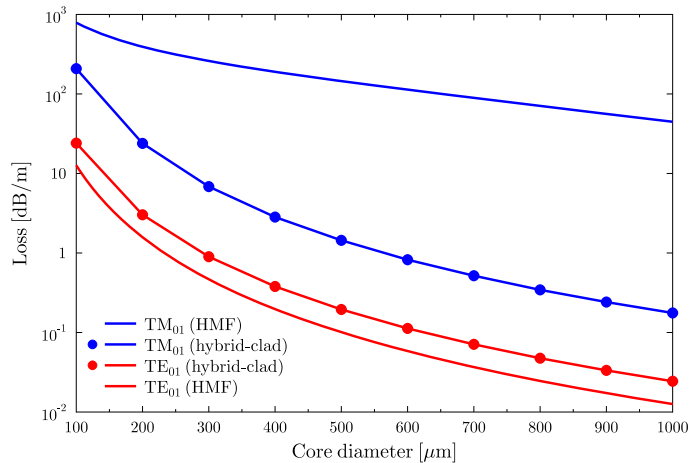


Fig. 8. Loss values for TE_{01} and TM_{01} modes guided by hybrid-clad fiber as a function of core diameter. The same curves for the full-metal fiber are also shown. $\lambda = 10.6\mu\text{m}$, $\Lambda = 2\mu\text{m}$, $f_m = 0.2$. The inner cladding has one layer of metal wires.

the TE propagation. However, we point out that, since the inner cladding is transparent to TE wave, it can give rise to constructive wave resonance in the layer. In turn, resonances can amplify the loss caused by metal-wire absorption. This resonance condition is fulfilled when the metamaterial thickness is equal to multiple of the half transverse-wavelength for TE light in the medium, which is confirmed numerically (not shown here).

In Fig. 8, we show how loss values of the TE_{01} and TM_{01} modes guided in a hybrid-clad fiber vary with respect to the fiber core size. As the core radius R increases, the losses decrease roughly as $1/R^3$. Such a loss dependence on R is also found for other types of hollow-core waveguides, including HMF [16] and the Bragg fiber [17]. In Fig. 8 we also show the loss values of the same two modes guided in a HMF. By comparison, we see that propagation loss for the TM mode is greatly reduced with our hybrid-clad design (by more than 100 times when core diameter is moderately large), whereas the loss for TE mode experiences only a slight increase.

MP modes have both TE and TM field components and the two sets of field components are not independent. Through numerous simulations, we have found that a MP mode with a low azimuthal order number in general has a propagation loss in between that of the TE_{01} and TM_{01} modes. In addition, the loss of a MP mode is somewhat closer to that of the TE_{01} mode. For example, for a fiber with a $700\mu\text{m}$ core diameter, the MP_{11} has a loss of 0.11 dB/m , and the MP_{21} mode has a loss of 0.28 dB/m . From Fig. 8, losses for the TE_{01} and TM_{01} modes are respectively 0.07 dB/m and 0.52 dB/m . It is worth mentioning that the MP_{11} mode in a HMF with the same core size experiences a loss of 49 dB/m .

4. Comparison to HMF with dielectric coating

It has been a common practice to reduce the propagation loss of a HMF by further imposing a dielectric coating on its inner wall [1, 4]. Here we would like to briefly compare the performances between a dielectric-coated HMF and a metamaterial fiber. Since TE light sees the metamaterial layer as if it is a dielectric medium, the two fiber types under comparison should be more or less equivalent for guiding TE modes. The major difference lies in their guidances of TM modes. With the same materials deployed in the previous sections, we will show that

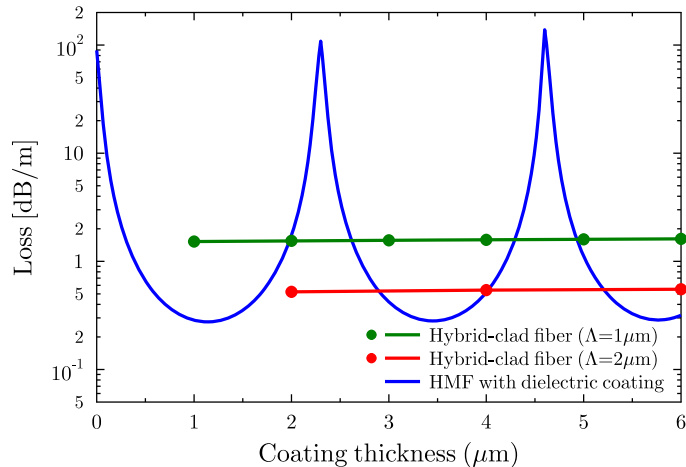


Fig. 9. Propagation loss for the TM_{01} mode as a function of coating thickness, for a HMF with dielectric inner coating and a hybrid-clad fiber incorporating metamaterial.

a HMF with a dielectric coating is able to perform slightly better than a metamaterial fiber in guiding TM_{01} mode. However, the former has the drawback of being quite sensitive to dielectric coating thickness, which on the other hand also implies its sensitivity to the operating wavelength.

Let us borrow the dielectric material previously used for the metamaterial host ($\epsilon = 6.25$) as the coating for a HMF. The HMF's outer cladding (silver) starts from a fixed value $r_2 = 350\mu\text{m}$. The first cladding interface is located at $r_1 = r_2 - d_c$ with d_c the coating thickness. We examine the propagation loss of the guided TM_{01} mode as a function of d_c . The result is shown in Fig. 9. When the coating thickness increases from 0 to $6\mu\text{m}$, the mode loss undergoes a periodic variation, with value ranging from 0.275 to over 100dB/m. This periodic change in loss is caused by the resonance and antiresonance of the dielectric layer. Therefore experimentally one has to locate an optimum coating thickness in order for such a fiber to work at a minimum loss [4]. Now, if we replace the dielectric coating with a metamaterial one, the periodic variation in modal loss can be suppressed. This is shown again in Fig. 9 by two flat curves, which correspond to two hybrid-clad fibers with different wire separations but with the same metal filling fraction at 20%. The independence of the TM modal loss to metamaterial coating thickness is an inherent result of the fact that the TM waves are evanescent in such a metamaterial. Hence practically the hybrid-clad fiber with metamaterial coating might be less sensitive to structural parameters, at least for the TM modes. We have also explored the possibility to further reduce the loss of the TM_{01} mode in a hybrid-clad metamaterial fiber by adding a second dielectric coating on top of the metamaterial layer. However, the further reduction in loss is not significant.

We should emphasize that the difference between the two types of fibers is far more complicated than what has been presented by Fig. 9. For example unlike TM modes, TE modes in the hybrid metamaterial fiber should have a periodic loss dependence on the coating thickness. That is, the two types of fibers have similar performances for guiding TE modes. Comparison of the MP modes between two types of fibers would be more intriguing. Since a MP mode comprises both TE and TM wave components, such modes in both fibers will be sensitive to their coating thickness. Some difference should however be expected because of the fibers' different guidance behaviors for the TM wave components. Due to significantly heavier computing resources required for numerically deriving the MP modes, an explicit comparison for guidances of MP

modes by the two types of fibers is not presented here.

5. Discussion and conclusion

Although our presentation has focused on the CO₂ wavelength, simulations were also carried out for other fiber structures based on silver and silica materials designed to operate at 1.55 μm wavelength. Very similar improvement in TM mode guidance for a hybrid-clad metamaterial fiber compared to a metal-clad fiber is noticed. However, due to the inherently huge Ohmic absorption of silver at this wavelength, propagation loss for the TM₀₁ mode in a hybrid-clad fiber, e.g. with a 30 μm core diameter, though reduced, can still be higher than 100 dB/m, which is hardly useful for practical applications. Hence with commonly accessible materials at disposal, the advantage of the proposed metamaterial fiber only becomes obvious at IR frequencies.

In conclusion, we have shown that a metal-wire based metamaterial functions as a TM reflector. The reflectance from a substrate made of such a metamaterial can be better than that from a plain metal at large incidence angles. Numerical simulations show that a hollow fiber with such a metamaterial cladding can easily propagate a TM mode 100 times farther compared to a simple HMF. With a hybrid-clad fiber which has a thin inner metamaterial cladding and an outer metal cladding, we can achieve low-loss propagation of modes in all categories. Such a fiber in theory can be as compelling as the state-of-the-art fibers, including the Bragg fiber and the more traditional HMF with a dielectric coating, for IR light delivery. We emphasize that the proposed guiding principle and in turn the fiber structure is within our fabrication capability at least in a foreseeable future. Our study also suggests that innovations in metamaterial technology can open many new possibilities for designing novel EM waveguides, especially for radiation frequencies previously considered problematic to transport.

Appendix

We derive the material requirement for wave confinements in a cylindrical hollow fiber as specified by Eqs. (6) and (7) in the text. We assume that the material parameters of the cladding have the tensor form as

$$\bar{\bar{\epsilon}} = \begin{pmatrix} \epsilon_r & 0 & 0 \\ 0 & \epsilon_\theta & 0 \\ 0 & 0 & \epsilon_z \end{pmatrix}, \quad \bar{\bar{\mu}} = \begin{pmatrix} \mu_r & 0 & 0 \\ 0 & \mu_\theta & 0 \\ 0 & 0 & \mu_z \end{pmatrix}. \quad (9)$$

Note that any tensor component can be a negative value. To simplify our analysis, we further assume $\epsilon_r = \epsilon_\theta \equiv \epsilon_t$ and $\mu_r = \mu_\theta \equiv \mu_t$. The harmonic dependence is taken as $\exp(-j\omega t + \beta z)$. Due to the cylindrical symmetry, field within the medium is completely characterized by two similar wave equations, one for H_z and the other for E_z. The H_z wave equation is

$$\frac{\partial^2 H_z}{\partial r^2} + \frac{1}{r^2} \frac{\partial^2 H_z}{\partial \theta^2} + \frac{1}{r} \frac{\partial H_z}{\partial r} + \frac{\mu_z}{\mu_t} k_t^2 H_z = 0, \quad (10)$$

where $k_t^2 = k_0^2 \mu_t \epsilon_t - \beta^2$. By variable separation $H_z = \Psi(r)\Theta(\theta)$, Eq. (10) can be decomposed into two equations. One of them gives rise to the angular dependence of the field as $\exp(im\theta)$, where m is an integer denoting the angular momentum number. The radial dependence of the field is governed by

$$\frac{\partial^2 \Psi}{\partial r^2} + \frac{1}{r} \frac{\partial \Psi}{\partial r} + \frac{1}{r^2} \left(\frac{\mu_z}{\mu_t} k_t^2 r^2 - m^2 \right) \Psi = 0. \quad (11)$$

Equation (11) is a Bessel or modified Bessel differential equation, depending on the sign of $\frac{\mu_z}{\mu_t} k_t^2$. For achieving light confinement in a hollow core, it is necessary for the field to be evanescent in the cladding while $\beta^2 < k_0^2$ (as wave should be propagating in the core). Subsequently,

we find that this condition can be fulfilled when

$$\frac{\mu_z}{\mu_t} (k_0^2 \varepsilon_t \mu_t - \beta^2) < 0 \quad (12)$$

and the corresponding radial eigen-field in the cladding can be written generally in modified Bessel functions as

$$\Psi = \mathcal{A} I_m(\tilde{k}_t r) + \mathcal{B} K_m(\tilde{k}_t r), \quad (13)$$

where $\tilde{k}_t = \sqrt{-\frac{\mu_z}{\mu_t} k_t^2}$. Similar analysis can be carried out for the E_z wave equation. And the resulted condition for the E_z confinement is

$$\frac{\varepsilon_z}{\varepsilon_t} (k_0^2 \mu_t \varepsilon_t - \beta^2) < 0. \quad (14)$$

The general radial wave solution is the same as Eq. (13) except with μ changed to ε . Other field components can be written as a function of E_z and H_z . Therefore once the conditions specified by Eqs. (12) and (14) are fulfilled, confinement of an overall mode can be ensured.

When $m = 0$, the six field components are divided into two unrelated groups giving rise to two types of angularly invariant modes: a TE mode group with field components H_z , E_θ , and H_r ; and a TM mode group with field components E_z , H_θ , and E_r . Therefore, Eq. (12) is the general guidance condition for TE modes, whereas Eq. (14) is the general guidance condition for TM modes.

Acknowledgement

This work is supported by The Danish Council for Strategic Research through the Strategic Program for Young Researchers (DSF grant 2117-05-0037).